Industrial Crops & Products 109 (2017) 498–508

Contents lists available at ScienceDirect

Industrial Crops & Products

journal homepage: www.elsevier.com/locate/indcrop

Assessing multi-scale deconstruction of wood cell wall subjected to mechanical milling for enhancing enzymatic hydrolysis

Jinxue Jiang[a,*], Jinwu Wang[b], Xiao Zhang[c], Michael Wolcott[a]

[a] Composite Materials and Engineering Center, Washington State University, Pullman, WA, 99164, USA
[b] Forest Products Laboratory, US Forest Service, Madison, WI, 53726, USA
[c] Bioproducts, Science and Engineering Laboratory, Washington State University, Richland, WA, 99354, USA

ARTICLE INFO

Keywords:
Mechanical pretreatment
Cell wall ultrastructure
Cellulose structure
Accessibility
Enzymatic hydrolysis
Principal component analysis

ABSTRACT

The hierarchical structure of wood cell walls resulting from complex arrangement and distribution of the heterogeneous components is considered to impact significant impediment to enzymatic hydrolysis of cellulose for biofuels. In this work, micronized wood with significant cell wall ultrastructural deconstruction were effectively produced from ring and puck milling within 12 min. In a subsequent enzymatic hydrolysis, micronized wood resulted in increase of cellulose hydrolysability by 4–14 folds over that of starting material. The underlying mechanism towards facilitating enzymatic hydrolysis was studied through delineating the ultrastructural changes and alternation of cellulose chemistry in micronized wood cell wall using SEM, TEM, CLSM, GPC, XRD, HPLC and Simon's staining techniques. Electronic microscopy revealed distinct stages of wood cell wall deconstruction that was coincident with particle size reduction, including cell fracture and delamination, cell wall disintegration, and amorphization of cell wall fragments. Simons' staining results also indicated increasing substrate accessibility and porosity of micronized wood, likely due to the ultrastructure alternation of cell walls. GPC and XRD revealed significant decrease of cellulose degree of polymerization (DP) and crystallinity. The correlation of these factors with cellulose hydrolysability was studied and further arranged in order through principal component analysis. The major positive factors affecting hydrolysability were surface accessibility and porosity, while cellulose crystallinity and DP were the major negative factors accompanied by particle size. The established weighed order of factors behind hydrolysability provides insights of lowering cell wall structural recalcitrance by mechanical manner.

1. Introduction

Lignocellulosic biomass offers the most abundant and the cheapest carbon source on the earth with the form of biopolymers in its cell wall (Zhao et al., 2012). Due to increasing depletion of fossil resource and serious environmental issues, considerable interest has emerged in converting lignocellulosic biomass into fossil fuel alternatives to create a diverse and economically viable renewable portfolio for fuels and chemicals. One feasible biomass conversion route is the depolymerization of cell wall polysaccharides with hydrolytic enzymes, followed by fermentation of intermediate sugars to alcohols or hydrocarbons by specific microorganisms (Himmel et al., 2007; Zhao et al., 2012). However, plant cell walls have a hierarchical architecture resulted from complex interactions of these biopolymers, making the biomass difficult to deconstruct (Himmel et al., 2007). Therefore, pretreatment is recognized as a necessary step to overcome the recalcitrance and make cell wall polysaccharides more susceptible and amendable to hydrolytic action by enzymes for maximizing the release of fermentable sugars (Himmel et al., 2007).

Pretreatment has been found to improve enzymatic hydrolysis of biomass by creating changes in substrate chemistry, structure and morphology. These changes include but are not limited to crystallinity, degree of polymerization, specific surface area, and lignin distribution, which result in increasing accessibility of the cell wall polysaccharides to hydrolytic enzymes (Chundawat et al., 2011a,b; Yang et al., 2011). Several thermochemical approaches (e.g. acid, alkaline, acid sulfite pulping, organosolv pulping, steam explosion, and ionic liquid pretreatments, etc.), have made substantial progress in facilitating enzymatic hydrolysis of pretreated biomass substrates through depolymerizing and/or partial removal of the cell wall non-cellulose constitutes (Bali et al., 2015; Del Rio et al., 2011; Foston and Ragauskas, 2010; Tadesse and Luque, 2011b; Zhu et al., 2009). However, these severe chemical processes often carry high capital cost, employ chemicals and solvents, and that require recovery or treatment of liquid stream may

* Corresponding author.
E-mail address: jinxue.jiang@wsu.edu (J. Jiang).

http://dx.doi.org/10.1016/j.indcrop.2017.09.009
Received 9 May 2017; Received in revised form 1 September 2017; Accepted 8 September 2017
Available online 12 September 2017

lead to formation of inhibitors to down-stream microorganism metabolism to produce desired fuels or chemicals. These challenges pose significant barriers to commercializing an economically viable biomass conversion process to fuels and chemicals (Barakat et al., 2014). Mechanical milling pretreatment offers an attractive alternative to address these deficiencies by producing digestible biomass substrates with the advantages of eliminating chemicals/solvents and the formation of inhibitors typically originated from degrading and/or transforming non-cellulose components (i.e. hemicellulose and lignin) in chemical pretreatment processes (Barakat et al., 2013).

The mechanical milling process is an effective strategy to break down the robust cell wall structure of woody biomass feedstock. It has long been used to deconstruct the native structure of plant cell wall for improving substrate accessibility, which enables providing the milled wood lignin (Fujimoto et al., 2005; Goundalkar et al., 2014; Maurer and Fengel, 1992). The milling process profoundly imparts multiple length-scale structural alternations (e.g., plant, tissue, cellular and molecular levels) through disrupting supramolecular cross-links of cellulose-hemicellulose-lignin networks (Ji et al., 2016). Studies in different laboratories have demonstrated that mechanical milling facilitates enzymatic hydrolysis of various feedstock (i.e., herbaceous and woody biomass) (Barakat et al., 2014; Takahashi et al., 2013; Vaidya et al., 2016; Zakaria et al., 2014). Silva et al. (2012) has indicated that destruction of cell wall to micronize-size range is essential for high glucose yield of mechanically milled wheat straw. The improvements may occur in tandem with decreases in particle size and cellulose crystallinity in milled substrates, which are associated with increased enzyme accessibility to cell wall polysaccharides. Our prior work (Jiang et al., 2016) has demonstrated that partial breakage of softwood fiber and/or fiber bundles improves the enzymatic hydrolysis of milled softwood, resulting in limited total sugar yields of around 40%. Mechanically disintegrating the fiber cell wall into micronized fragments significantly improves the enzymatic hydrolysis, with total sugar yields of over 70%. Similarly, Ji et al. (2016) also found that mechanically fragmenting corncob samples at a cellular scale resulted in a 98.3% conversion yield of cellulose to glucose. In addition, decreasing the cellulose crystallinity during the milling process also contributes to increasing accessibility to cellulose microfibrils (Wang et al., 2014). Substantial research reveals a strong correlation between increased enzymatic hydrolysis efficiency and decreasing crystallinity in various milled feedstock (Barakat et al., 2014). Despite the demonstrated efficiency of mechanical milling pretreatment for disrupting the cell wall structure and increasing enzymatic hydrolysis yields, a clear understanding of the ultrastructural alternation and cellulose characteristics that are presumably responsible for facilitating enzymatic digestion and revealing biomass recalcitrance is still needed. On the other hand, studies on evaluating the relative importance of the different structural factors to the hydrolysability of milled biomass has not been elucidated, while most reports have only focused on correlations of hydrolysability with physicochemical characterizations.

The objective of this study is to delineate the effects of mechanical milling pretreatment on the ultrastructural properties and cell wall chemistry of micronized wood as related to the sugar release efficiency or recalcitrance properties of biomass. Specifically, the physicochemical changes resulting from the mechanical deconstruction of softwood Douglas-fir (*Pseudotsuga menziesii*) feedstock have been examined by using combined wet chemistry techniques with other analytical and imaging techniques in new ways. Transmission electron microscopy (TEM) was used to investigate the ultrastructural disintegration of the wood cell wall and, as it turned out, to reveal the increased substrate accessibility and porosity within the cell wall fragments. Confocal laser scanning microscopy (CLSM) was employed to delineate the distribution of chemical composition related to breakdown of cell walls during the milling process. Enzymatic hydrolysis experiments on micronized wood was also conducted in an effort to assess the change in the recalcitrance of milled substrates. In addition, statistically quantifying the relative importance of different structural and morphological factors on enzymatic hydrolysis efficiency provides insights into the fundamental nature of cell wall recalcitrance related to enzymatic hydrolysis efficiency of lignocellulosic biomass.

2. Materials and methods

2.1. Materials

Clean, Douglas-fir (*Pseudotsuga menziesii*) wood chips were obtained from a local company (Vaagen Brothers Lumber Inc., Colville, WA). The as-received chips were separated by a vibrating screen with 25.4-mm aperture and pre-ground into particles by a hammer mill fitted with a 3.18-mm screen. The pre-ground feedstock was subsequently conditioned to a target equilibrium moisture content of 5% (dry weight base). Before further mechanical pretreatment, the conditioned sample was stored in sealed plastic bag and the moisture content was validated using gravimetric methods according to standard protocol (Sluiter et al., 2008a).

2.2. Mechanical pretreatment process

Mechanical milling pretreatment was performed using a high-energy vibratory ring and puck mill with motor power of 1.1-kw (Rocklab Pty Ltd, New Zealand). The sample (10-g, oven-dry base) was milled in a chamber with an inner diameter of 128-mm and height of 43-mm along with a ring (78-mm inner diameter, 100-mm outside diameter, 41-mm height) and a puck (52-mm diameter and 41-mm height) as the milling media. Both the milling chamber and grinding media were made of tungsten carbide. Milling process was conducted for a total time of 2–12 min, with 2-min intervals, resulting in particles in micrometer range. Thus, the milled samples were also noted as micronized wood (or micronized particles) here.

2.3. Enzymatic hydrolysis

Enzymatic hydrolysis experiments were performed using Cellic CTec2 cellulase (15 FPU/OD g of substrate) and cellic HTec2 hemicellulase (1/9 of the cellulase amount). Digestion was carried out in 125-mL flasks with a citrate buffer (pH 4.8) at a solid loading of 2%. The flasks were settled in an incubator with a rotation speed of 180rmp at 50 °C. After digestion for 72 h, the hydrolysate was analyzed by HPAEC. Glucan and xyl/mannan conversions were defined as the percentage of glucose and xyl/mannose that was released in enzymatic hydrolysate compared to the theoretical maximum.

2.4. Composition analysis of the wood samples

The chemical composition analysis of wood material was conducted according to the two-step acid hydrolysis procedures from the NREL standard protocol (Sluiter et al., 2008b). Briefly, a 300-mg sample and 3-mL of 72% H_2SO_4 was added to a 100-mL pressure tube, and incubated at 30 °C for 1 h and stirred every 15 min. The sample was then diluted with 84-mL deionized water and autoclaved for one hour. Detection of sugars was performed with high-performance anion exchange chromatography (HPAEC) (Dionex, ICS-3000). The acid soluble lignin content was determined by UV–vis spectrophotometer (Lambda 25, PerkinElmer), while the solid residue in during acid hydrolysis process was counted as insoluble lignin. The total lignin content is the sum of acid soluble and insoluble lignin.

2.5. Structural characterization of micronized wood samples

2.5.1. Scanning electron microscopy (SEM)

Micronized wood samples were mounted on aluminum stubs using carbon tape and sputter-coated with 8-nm of gold for good conductivity

prior to imaging. Imaging by SEM was performed using an FEI Quanta 200F field emission gun with high vacuum ETD detectors (FEI Company, Hillsboro, Oregon, USA). Imaging was taken at beam accelerating voltage of 20-kV.

2.5.2. Particle size measurement

The volumetric particle size distribution of the micronized wood was determined using a laser scattering particle size analyzer Mastersizer 3000 with Hydro LV wet sample dispersion (Malverninstrument, UK). The median size (D_{50}) was used to represent theparticle size for analysis.

2.5.3. Sample embedding and sectioning

Wood samples were processed using microwave electronic microscopy processing methodology as described elsewhere (Donohoe et al., 2008). Briefly, samples were fixed in 3% glutaraldehyde and buffered in 0.05-M Pipes buffer (Sigma, St Louis, MO) with a microwave oven. The samples were dehydrated in graded ethanol series (i.e., 30%, 50%, 60%, 70%, 80%, 90%, and 3 × 100% ethanol) in a microwave oven. The samples were then infiltrated with Spurr's resin and incubated overnight at room temperature in a hood with increasing concentrations of the resin (i.e., 30%, 50%, 3 × 100% resin, diluted in isopropanol). The samples were transferred to micro-centrifuge tubes and the resin polymerized overnight at 70 °C. The embedded samples were sectioned to 300 nm for light microscopy and to approximately 100 nm for TEM using a Diatome diamond knife on a Leica Reichert Ultracut R microtome (Leica, Wetzlar, Germany).

2.5.4. Confocal laser scanning microscopy (CLSM)

The composition distribution in micronized wood was characterized by using confocal laser scanning microscopy (CLSM) as detailed elsewhere (Jiang et al., 2017a; Yu et al., 2014). Semi-thin (300 nm) samples were positioned on glass microscope slides and stained with saturated HPLC-grade acridine orange (AO; 3, 6-bis (dimethylamino) acridine hydrochloride, Sigma-Aldrich, St. Louis, MO) for one hour at room temperature. After staining, the samples were washed three time with DI water. The imaging of stained samples was performed using a Leica TCS SP8 with a 40 × oil objective lens. A white laser at wavelength of 500 nm was used as the excitation light source. Fluorescence emission in the 515–540 nm spectral region were acquired as the green channel, and emissions above 590 nm spectral region were collected as the red channel. Image analysis was performed using LAS AF Lite imaging analysis software. Color in green represented area rich in carbohydrates, while lignin was represented by red color. Furthermore, multiple line scans across cell walls and wall fragments were also analyzed to investigate the lignin/carbohydrates redistribution. The signal intensity represented as raw pixel intensity and distance as the pixel distance.

2.5.5. Transmission electron microscopy (TEM)

Ultrathin sections were placed on Formvar coated copper slot grids (SPI Supplies, West Chester, PA). Grids were post-stained for 10 min with 1% w/v $KMnO_4$ to selectively stain for lignin. TEM imaging were taken with a 4 megapixel Gatan UltraScan 4 K Eagle camera (Gatan, Pleasanton, CA) on a FEI Tecnai G2 20 Twin 200 kV LaB6 TEM (FEI, Hilsboro, OR).

2.5.6. Gel permeation chromatography (GPC) analysis of cellulose

The molecular weight distribution of cellulose in micronized wood was determined by GPC after benzylation of α-cellulose that enables cellulose to be dissolved in tetrahydrofuran (THF) (Leskinen et al., 2011; Zoia et al., 2011). Isolation of α-cellulose was obtained by delignifying wood samples with sodium chlorite/acetic acid, and then through alkaline extraction of holocellulose following the prcedures elsewhere (Yokoyama et al., 2002). Benzoylation of α-cellulose was conducted according to previously established procedures (Zoia et al., 2011). Prior to GPC analysis, benzoylated samples were dissolved in THF (1 mg/mL), filtered through a 0.45-μm membrane, and placed in a 2-mL auto-sampler vial. Size-exclusion separation was performed on a Viscotek gel permeation chromatograph system equipped with a GPCmax™ unit and a TDA 305 multidetector unit using THF as the mobile phase. One AM Gel 100/5 column (American Polymer Standards Corporation) and two MBHMW-3078 columns (300 × 7.8 mm, Malvern) were used. The temperature of column oven was 30 °C and the injection volume was 100 μL. A calibration curve was constructed based on 8 polystyrene standards, each with narrow ranges in molecular weight from 2.2 to 3600 kDa. The number-average degree of polymerization (DP_n) and weight-average degree of polymerization (DP_w) were obtained by dividing M_n and M_w respectively by 162 g/mol. All reported values were the mean average of duplicate samples.

2.5.7. Determination of cellulose reducing ends

The amount of cellulose reducing ends (μmoles/g wood) was determined by DNS assay. The DNS reagent was prepared by mixing 1416-mL distilled water, 10.6-g 3, 5 Dinitrosalicylic acid and 19.8-g sodium hydroxide, following the addition of 306-g Rochelle salts (sodium potassium tartrate), 7.6-mL phenol (melt at 50 °C) and 8.3-g sodium metabisulfite, as noted in a technical report (Adney and Baker, 1996). About 1.5-mL of sample slurry containing 50-mg wood in distilled water was added into the test tubes and followed by adding 3-mL freshly made DNS reagent. The tubes along with duplicate anhydrous glucose calibration standards (2–6.7 mg/mL) were boiled for 5 min in a vigorously boiling water bath. After boiling, tubes were transferred to a cold ice-water bath. Color formation of the supernatant was measured at 540 nm with a UV–vis spectrophotometer (Lambda 25, PerkinElmer), and the amount of cellulose reducing ends was determined from absorbance calibration plots generated for standards.

2.5.8. Cellulose crystallinity

X-ray diffractograms of the micronized wood particles were obtained using a powder x-ray diffractometer (Rigaku, Miniflex 600, Japan) with a Cu Kα (λ = 0.154 nm) radiation source generated at 40-kV and 15-mA. The instrument scanning range 2θ was from 10 to 40° with a step size of 0.02° every 0.5 s. The relative degree of cellulose crystallinity, in terms of crystallinity index (CrI), was estimated using equation as described by Segal (Segal et al., 1959):

$$CrI = \frac{I_{002} - I_{am}}{I_{002}} \times 100\%$$

where I_{002} is the intensity of main peak, and I_{am} is the intensity due to amorphous portion evaluated as the minimum intensity between the main and secondary peaks.

2.5.9. Simons' staining for measurement of substrate accessibility

The Simons' staining was carried out to assess the substrate accessibility of micronized wood according to published procedures elsewhere (Chandra et al., 2008). Direct Blue 1 (DB) (Pontamine Fast Sky Blue 6BX) and Direct Orange 15 (DO) (Pontamine Fast Orange 6RN) dyes were obtained from Pylam Products Co. Inc. (Garden City, NY). DB was used as received, while DO was separated by 10 K membrane using the Amicon ultrafiltration apparatus (Amicon Inc., Beverly, MA) under pressure of 35-psi. The purpose of fractionation of high molecular weight DO is to ensure its absorption to represent enzyme (Ju et al., 2013). This is because only high molecular weight fraction of the DO dye is responsible for the increased affinity for cellulose. Wood samples (100-mg, oven dry base) were weighed into six centrifuge tubes with a 1.0-mL phosphate buffer saline solution (pH 6, 0.3-M PO_4, 1.4-M NaCl). The same amount of 1% dye solution of DB and DO were added to each of the six tubes with increasing volumes (0.25, 0.5, 0.75, 1.0, 1.5, 2.0 mL). Next, distilled water was added to each tube to bring the final volume to 10.0 mL. After incubation at 70 °C for 6 h with shaking at 180 rpm, the slurry was separated by centrifugation. The absorbance of

the supernatant was measured at wavelength of 455 nm and 624 nm with a UV–vis spectrophotometer (Lambda 25, PerkinElmer). Each dye concentration in the supernatant was obtained by solving two Lamber-Beer law equations simultaneously. Each dye adsorbed by the wood substrate was accounted with the difference between the concentration of the initial dye and the dye in the supernatant. The maximum adsorption capacity of the two dyes were determined according to the Langmuir adsorption equation

$$\frac{[C]}{[A]} = \frac{1}{K_{ads}[A]_{max}} + \frac{[C]}{[A]_{max}}$$

where $[C]$ (mg/mL) is the free dye concentration, $[A]$ (mg/g) is the amount of dye adsorbed by the substrate, K_{ads} is Langmuir adsorption constant, and $[A]_{max}$ is the maximum amount of dye adsorbed.

The ratio between DO and DB adsorption capacities (DO/DB) was used as a measure of the large-to-small pore ratio of the material (Chandra et al., 2008).

2.6. Principal component analysis (PCA)

The importance of the effect of structural factors in enzymatic hydrolysis was quantified by PCA using Unscrambler Version 10.4 software (CAMO software, A/S, Oslo, Norway). The principal components are linear combinations of the original variables, especially the eigen values of the covariance matrix of the variables. In principal component regression, the components that account for the majority of variance in the data are used as variables. The data was z-normalized and the variables were transformed into principal components using PCA.

3. Results and discussion

3.1. Enzymatic hydrolysis of micronized wood

The main target of pretreatment is to overcome the recalcitrance of lignocellulosic substrates for efficient enzymatic hydrolysis of polysaccharides. Table 1 shows monosaccharide yield in enzymatic hydrolysis for micronized wood samples with various milling times. After mechanical pretreatment, the sugar yield of samples improved compared to the starting material. These results concurred well with the literatures, which claim that mechanical milling increases accessibility and digestibility of substrates for various herbaceous and woody biomass (Sipponen et al., 2014; Takahashi et al., 2013; Zakaria et al., 2014). In our study, the monosaccharide yield after enzymatic hydrolysis also increased with increased milling time. The highest glucose yield was around 90%, approximately 14 times higher than the yield of the starting material. To examine the enhanced sugar release, the cellulose chemistry and cell wall ultrastructure of micronized wood samples were explored in depth.

3.2. Chemical composition of micronized wood

Typically, changes in chemical composition of biomass after thermo-chemical pretreatments mostly contribute to increasing enzymatic hydrolysis of pretreated substrates (Harmsen et al., 2010). After mechanical pretreatment here, the bulk chemical composition of micronized wood remains unchanged regardless of milling times (Table 1). We note that others have found that ball milling for long periods (i.e., tens of hours or several weeks) may result in degradation of components in biomass cell wall (Holtman et al., 2006; Zoia et al., 2011). In our study, the ring and puck milling required much shorter milling time for satisfactory enzymatic sugar release without degradation of chemical components. The difference in sugar release of micronized wood with different milling times may be related to their morphological and structural alternations.

3.3. Particle morphology of micronized wood

In this study, we have examined the changes in the particle morphology for milled wood with increasing milling times by using scanning electronic microscopy (Fig. 1). Effectively micronized softwood was obtained using a ring and puck mill. A disrupted fiber structure was observed after 2-min of milling and is characterized by separated fibers/fiber bundles (arrows in Fig. 1A). The fiber fragments started to prevail after 4-min of milling, due to chopping and breakage of individual fibers (arrow in Fig. 1B). After 6 min, the fiber cell wall was almost entirely fragmented, resulting in sizes of ca. 20-μm. No further particle size reduction was observed with additional milling times up to 12 min, mainly due to aggregation effect. Laser diffraction analysis confirmed the particle size changes of micronized wood during the milling process (Fig. 1G & H), indicating deconstruction of ordered micro-scale cell wall structure by mechanical forces. Particle size is considered one of the important structural features that can affect the enzymatic digestibility by increasing the exposed external surface area, although the particle size reduction is not significant for micronized wood with longer milling time (Jiang et al., 2016). As one aspect of physical structural alternation, our results indicated that particle size changes in micronized wood facilitate hydrolysability of softwood, arguably the most recalcitrant of biomass types.

3.4. Chemical composition distribution of micronized wood

In this study, we applied confocal laser scanning microscopy (CLSM) with acridine orange-stained sections to explore the deconstruction phenomena of cell wall and redistribution of lignin in the cell wall. Acridine orange (AO) is used to stain the heterogeneous plant cell wall and its brightness has been reported to be proportional to lignin concentration (Li and Reeve, 2005; Zhang et al., 2012). When AO interacts with polysaccharides, it remains in a monomeric state, resulting in fluorescence emission in the green light region. However, when AO interacts with the aromatic π electrons in lignin, the electron density of the molecules will cause aggregation of AO molecules, leading to a fluorescence emission shift to red light spectrum (Yu et al., 2014). Line scans provide a more quantitative analysis of the changes in lignin distribution within the intact cell walls and variable cell wall fragments

Table 1
Chemical composition and theoretical enzymatic hydrolysis yield of micronized wood.

Milling time (min)	Chemical composition (mass percentage of the wood%)					Enzymatic hydrolysis yield (% of theoretical yield)		
	Glucan	Xyl/mannan	Galactan	Arabinan	Lignin	Glucose	Xyl/mannose	Total sugars
0	45.18	16.53	2.69	1.32	28.88	6.23	3.67	5.56
2	45.18	16.53	2.69	1.32	28.88	21.73	17.62	20.61
4	44.47	16.45	2.66	1.31	28.11	39.35	25.66	39.59
6	44.85	16.60	2.61	1.32	28.53	62.06	35.20	54.69
8	44.40	16.35	2.62	1.29	29.24	77.32	42.03	67.67
10	44.63	16.57	2.58	1.26	28.76	81.77	40.42	70.39
12	44.62	16.51	2.86	1.23	28.63	89.81	42.93	76.94

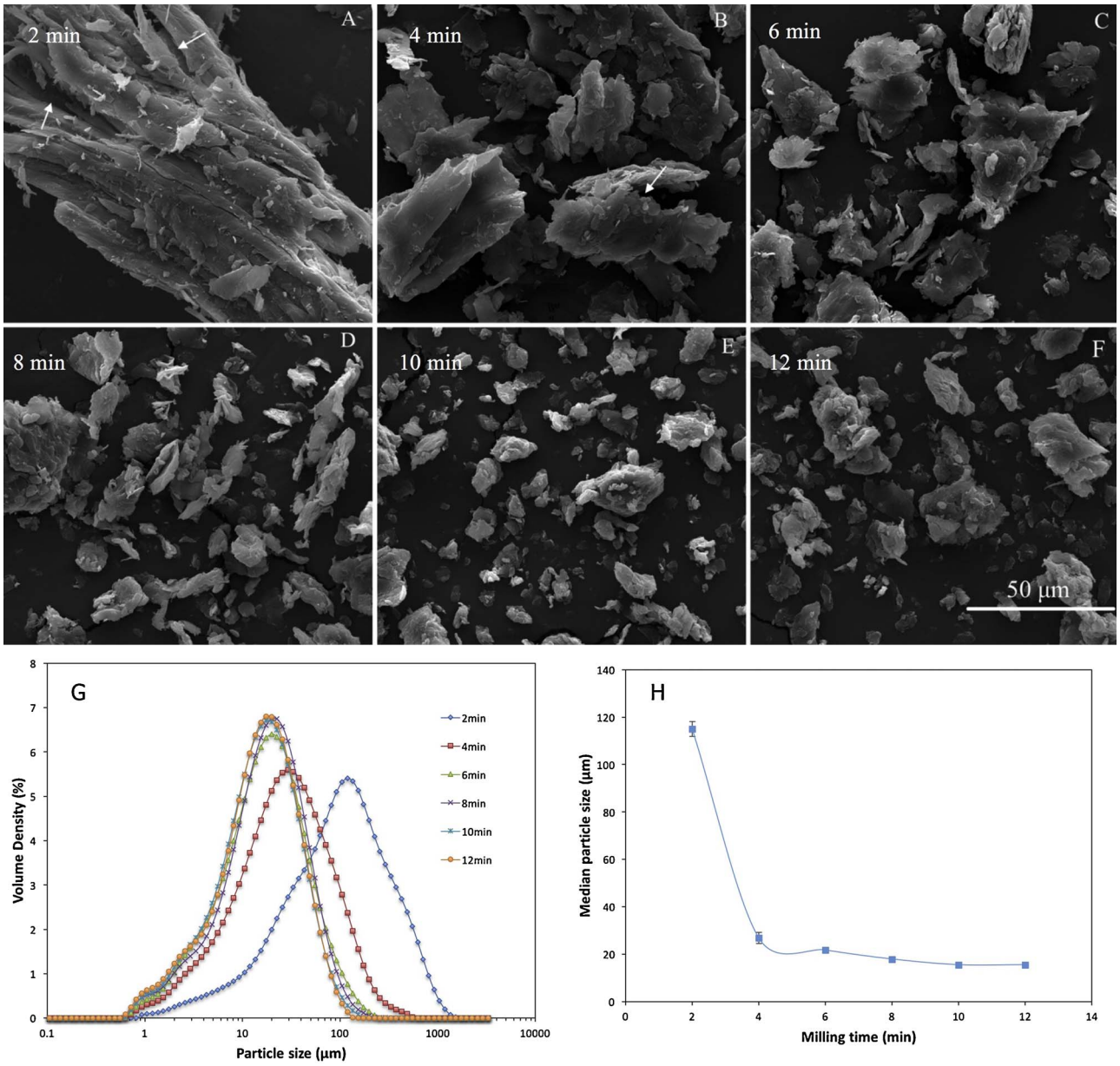

Fig. 1. SEM micrographs of micronized wood samples with various mechanical pretreatment times. Mechanical pretreatment caused tissue fracture with cell wall separation at the early stage (A, arrows). Further milling resulted in chopping and breakage of individual fibers (B, arrows). There was no noticeable change of particle morphology after total disintegration of the cell wall (C–F) due to aggregation effect. (G) Volume based particle size distribution, (H) median particle size as a function of milling time.

(Jiang et al., 2017a).

As anticipated, the raw material (Fig. 2A) shows a very uneven distribution of lignin across the cell walls, with lignin rich regions in the cell wall corner and middle lamella. In contrast, a strong green signal is visibly evident in polysaccharides-rich secondary cell wall layers (Fig. 2A). These observations are consistent with previous results reported elsewhere (Sant'Anna et al., 2013; Singh et al., 2009). Compared to the intact cell walls, lignin distribution changes dramatically along with the cell wall fracture. The densely packed middle lamella lignin becomes loosely distributed on the fracture surface as the fiber bundles are separated among the middle lamella of adjacent cell walls at a 2-min milling time (Fig. 2B). Fig. 2C illustrates that additional milling produces remarkable fragmentation of the cell wall structure along with the continuous lignin redistribution in the micronized fragments. After 12 min of milling, the lignin that once coated the cellulosic fibers is evenly distributed across the cell wall fragments (Fig. 2D). Fig. 2D also indicates the most uniform signal intensity of lignin and polysaccharides, respectively, suggesting that the physical barrier of lignin has been alleviated. Previous studies indicate that pretreated biomass with cellulose exposure resulted from microstructure changes in cell walls contributed increase of its enzymatic digestion (Jiang et al., 2017a; Ju et al., 2013). In this study, the chemical redistribution resulted from cell wall deconstruction by mechanical process is also believed to benefit the increased hydrolysability of micronized wood.

3.5. Ultrastructure changes in micronized wood

TEM micrographs of micronized particles exposed to increasing levels of mechanical pretreatment are shown in Fig. 3. Interpretation of ultrastructure changes in these micrographs reveals several stages of mechanical deconstruction of wood cell wall as outlined below.

(1) Intact Cell Walls − Representative cross and longitudinal sections are shown in Fig. 3A and B. In these sections, the secondary cell

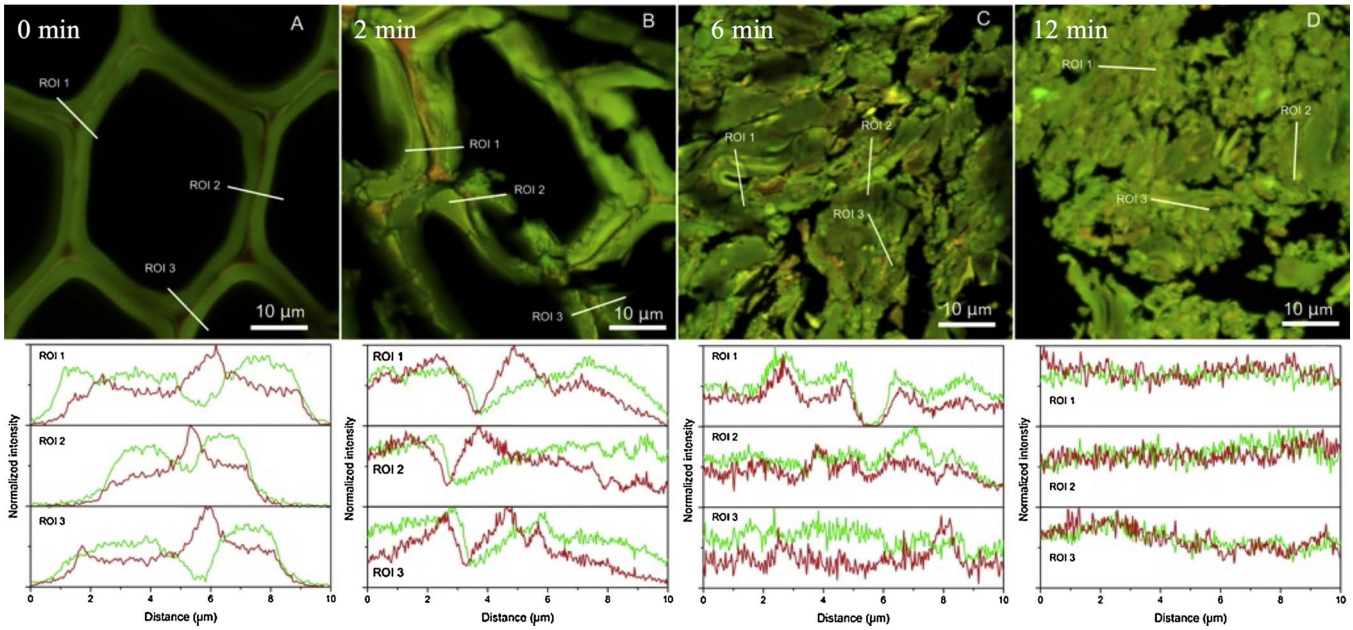

Fig. 2. Confocal laser scanning microscopy (CLSM) images of chemical composition distribution in raw and micronized wood. Across section of intact cell wall (A); sections of cell wall fragments with mechanical milling of 2 min (B); 6 min (C) and 12 min (D). Line scan profiles demonstrate that the distribution of lignin and polysaccharides changes along with the deconstruction of cell wall structure under intensive mechanical action. The red color indicates lignin and green indicates polysaccharides. ROI: region of interest. (For interpretation of the references to colour in this figure legend, the reader is referred to the web version of this article.)

walls (S1, S2 and S3), compound middle lamella (CML) and cell wall corners (CC) are clearly evident. Coarse milling produces particles in this stage, likely due to mechanical action on plant tissue separation with maintaining intact cell wall.

(2) Cell Fracture and Delamination – After 2–4 min of milling time (Fig. 3C and D) cell fractures in the CML and CC become prevalent. Fractures progress to larger scale delamination and eventual cell wall fragmentation as evident in Fig. 3D. Combined, these processes serve mainly to separate adjacent cells and reduce particle size, while largely maintaining the original cell wall ultrastructure.

(3) Cell Wall Disintegration – Fig. 3E and F reveal that additional milling results in disintegration of cell wall ultrastructure, displaying a total collapse of orderly structural cell wall and randomly generating multiple cell wall fragments. These fragments are difficult to assign to specific cell wall locations. The longer the milling time, the higher the degree of ultrastructural disruption.

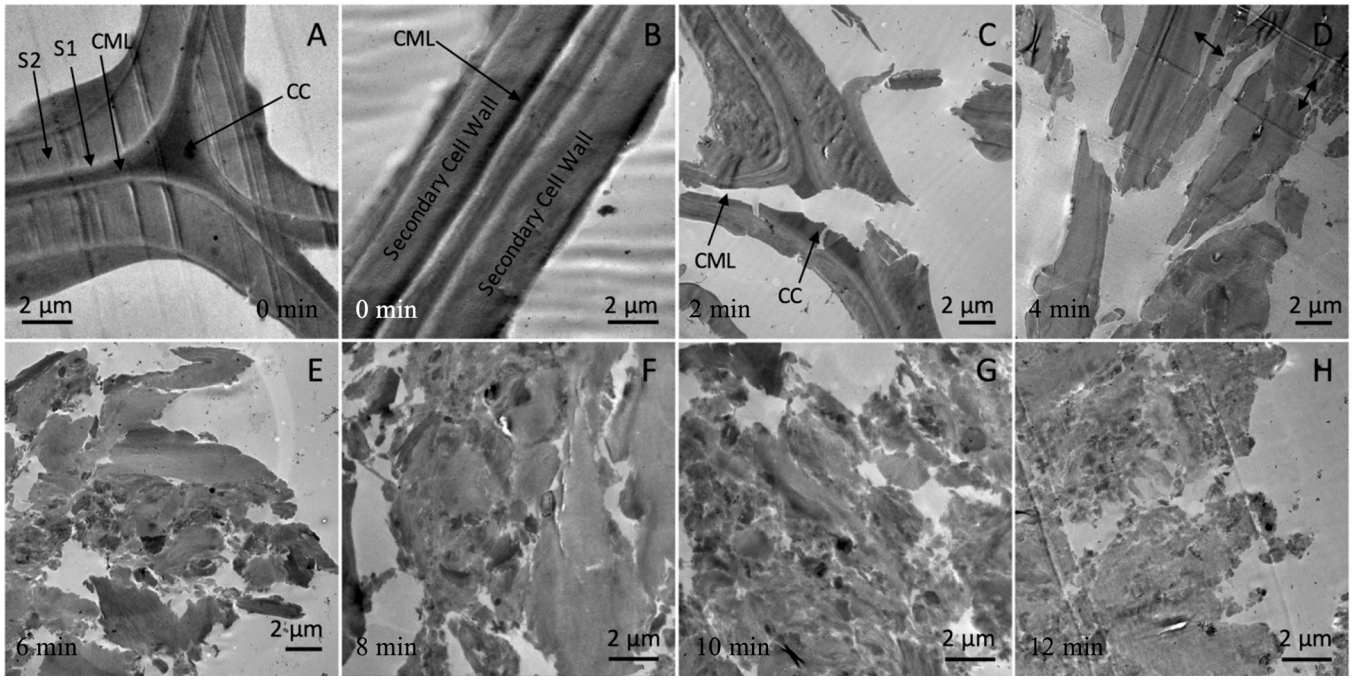

Fig. 3. TEM micrographs with low magnification reveal progressive cell wall deconstruction produced with different mechanical pretreatment times. Representative cross (A) and longitudinal (B) sections display cell wall hierarchical characteristics with multiple cell wall layers. Cell fracture and delamination (C and D) are resulted from short milling times of 2–4 min. Additional milling cause disintegration of cell wall altrastructure, generating various cell fragments (E and F). The last milling stage mainly involves cell fragments amorphization, presenting uniform nanoscale aggregates (G and H).

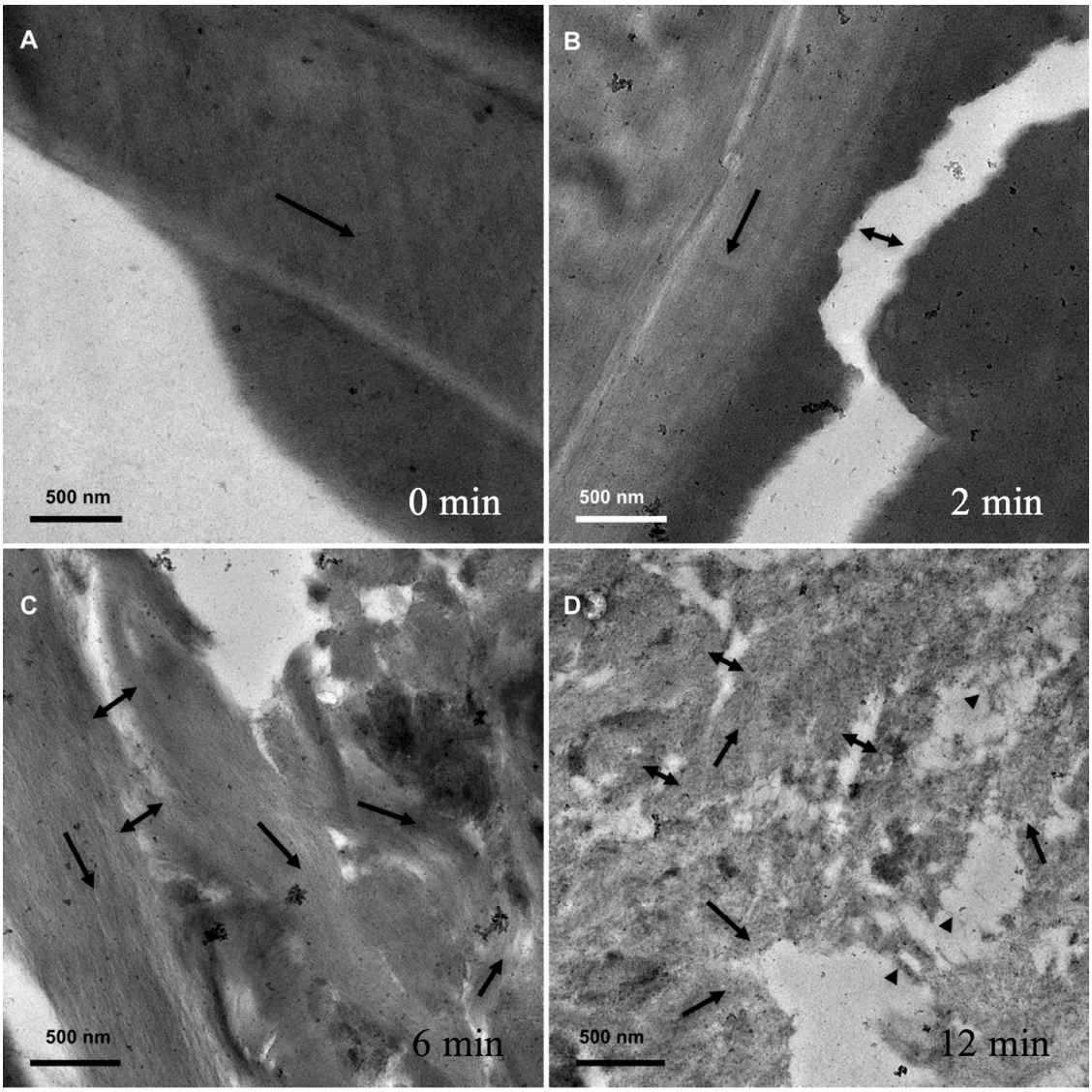

Fig. 4. TEM micrographs with higher magnification display disruption of microfibrils network along with structural cell wall deconstruction produced with different milling times. Arrows show orientation of cellulose microfibrils in intact cell wall and cell wall fragments. Double headed arrows show microfibrils delamination and intra voids. Arrow heads show microfibrils nanoscale aggregates.

(4) Cell Fragments Structure Amorphization − The final milling stage is characterized as amorphization of cell wall fragments (Fig. 3G and H). This generates aggregates that are largely agglomeration to nanoscale particles with a much more amorphous structure than the samples with shorter milling times.

It is conceivable that generating various cell wall fragments under mechanical action would also disorder and disorient the cellulose microfibrils. TEM images with higher magnification (Fig. 4) of the micronized wood visualize the disruption of microfibrils network from these milling stages. Fig. 4A shows the dense and solid cell wall with highly packed cellulose microfibrils network in the raw material. At the early milling stage, the densely ordered mirofibrils is still visibly evident (Fig. 4B), since fractures mainly occurred in the CML and CC regions. Sample that was milled for 6 min produce complete disintegration of the cell wall and show disorientation in the microfibrils of cell wall fragments (Fig. 4C). Delamination of the microfibrils is also visibly evident in this sample, producing additional internal porosity (Fig. 4C). Disintegrating the cellulose microfibrils with various nanoscale aggregates (Fig. 4D) is found in the microfibrils network for samples milled for 12 min. Fig. 4D also indicates that disrupting the cellulose microfibrils network resulted in various intra-particle voids (Fig. 4D). The difference in sugar yields of micronized wood samples in present study highlights the importance of complete collapse of hierarchical ultrastructure and further disruption of microfibrils network in cell wall fragments for facilitating hydrolysability of wood after mechanical pretreatment.

3.6. Molecular structure changes in micronized wood cellulose

One of the important recalcitrant factors influencing enzymatic hydrolysis is related to the cellulose molecular structure, namely molecular weight. To determine the potential influence of mechanical pretreatment on the cellulose structure, the average degree of polymerization of benzoylate derivatized α-cellulose isolated from micronized wood as analyzed by GPC (Table 2). The data clearly shows that the molecular weight of micronized wood cellulose decreases as milling time increases. Compared to the starting material, the DP_n of a sample milled for 2-min decreases by 17%, with additional milling, the decrease in DP_n continues, reaching a 73% decrease in sample milled for 12-min. Liimatainen et al. (2011) previously reported similar results of decreasing DP for cellulose microfibers after wet-stirred media milling.

Table 2
Molecular characterization of micronized wood samples.

Milling time (min)	DP_n	DP_w	PDI (M_w/M_n)	Reducing ends (μmoles/g)	CrI (%)
0	1068	5460	5.1	16.64	52.3
2	891	3953	4.4	20.22	47.9
4	565	3450	6.1	28.48	30.8
6	429	2484	5.8	37.46	22.6
8	398	1705	4.3	43.22	17.3
10	324	1228	3.8	50.11	11.9
12	293	1368	4.7	53.96	8.9

DPw = weight-average degree of polymerization, DPn = number-average degree of polymerization, PDI = polydispersity index, CrI = crystallinity index. Each result is the average of duplicate samples.

In their study, DP values decreased by about 75% after 15- or 35-min milling, depending on the amounts of milling media used. It is likely that decreasing molecular weight in cellulose is seldom an independent result after mechanical milling of lignocellulosic biomass. Breakage of the molecular chain collectively results in a decrease of particle size and cellulose DP. Ju et al. (2013) also reported significant difference in DP of kraft pulping fibers after fractionating in a Bauer-McNett fiber classifier fitted with different mesh screens.

Cellobiohydrolase I (Cel7A) plays vital important role in hydrolyzing cellulose, since it can attack the reducing ends to remove a molecular strand of cellulose with more internal sites exposure (Ganner et al., 2012). Therefore, it is commonly thought that reducing ends influence the rate and extent of enzymatic hydrolysis of cellulose. In this study, we examined the effect of mechanical milling on the total number of reducing ends using DNS assay, in which 2-hydroxy-3, 5-dinitrobenzoic acid reacts with the reducing ends and accompany color formation (Miller, 1959). In Table 2, the number of reducing ends increases from 16.64 μmol/g for a starting sample to 51 μmol/g for the sample with 12 min of milling. A previous study also claimed that milled wood samples with various vibrational milling time had increased carbonyl groups, which were quantified by the copper number (Mikushina et al., 2002). The increase in reducing ends agrees with the results discussed previously, specifically the decrease in cellulose DP during mechanical milling, mainly due to fragmentation of cellulose chains.

The effects of mechanical pretreatment on the crystalline structure of wood cellulose as measured by XRD are shown in Fig. 5. The X-ray diffraction patterns show typical peaks of cellulose I, with a gradual decrease in crystalline ordering as milling time increased. Crystallinity index (CrI) values decreased from 52% for raw material to around 9% for micronized wood with 12 min of milling (Table 2). With the longest milling time, the sample showed a broad peak at approximately 2θ = 21°, suggesting that the material was in a largely amorphous state. The decrease in CrI may be due to the fragmentation of crystalline grains, deformation of the crystalline structure, promoting an increase in amorphization during the mechanical pretreatment. Similar CrI changes as a function of milling time have been previously reported for diverse biomass feedstock (Barakat et al., 2014). Collectively, the XRD spectra and CrI values confirmed the disruption of the crystalline structure, which facilitates accessibility for enzyme attack. In our study, there was no transformation of the cellulose I structure into the cellulose II allomorph, which has been previously found for ball milling of pure cellulose in wet media (Nge et al., 2013).

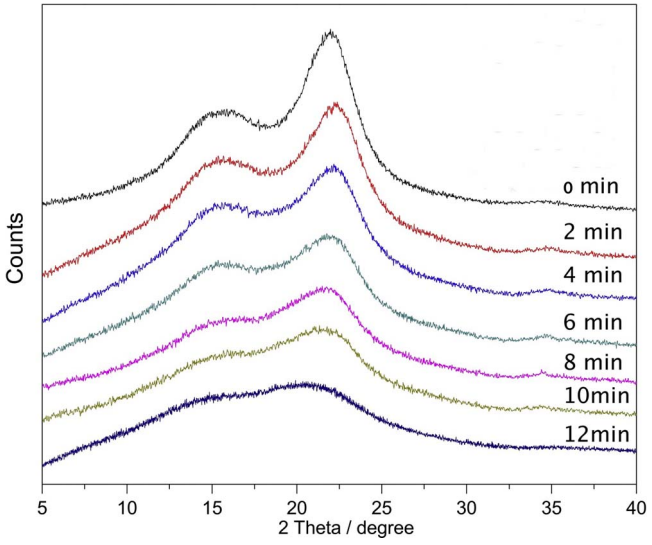

Fig. 5. X-ray diffraction patterns of micronized wood from various mechanical pretreatment times. Amorphization of crystal cellulose occurs as milling time increases.

3.7. Accessibility of micronized wood as measured by Simons' staining

The Simons' staining technique has been shown to be a semi-quantitative method for characterizing the accessible features of lignocellulosic biomass with two color differential dye probes (i.e., Direct Orange 15 and Direct Blue 1) (Chandra et al., 2008). The molecular diameter of Direct Blue 1 (DB) is approximately 1 nm, while the molecular diameter of Direct Orange (DO) ranges 5–36 nm for the high molecular weight fraction (which has higher binding affinity to the cellulose hydroxyl group than does DB) (Yu et al., 1995). Therefore, competing phenomena occur in the treatment of lignocellulosic substrates with a mixed dye solution of DO and DB molecules. In other words, the DB probes enter the smaller pores (diameter around 1 nm), while DO molecules will occupy the larger substrate pores or surface. The ratio between the maximum adsorption of DO to DB dyes on the substrates is therefore a good indicator of large-to-small pore ratio, which is also considered as the porosity of substrates (Chandra et al., 2008). Moreover, the hydraulic diameter of cellulase is approximately 7 nm, thus, DO adsorption has been proposed to assess the cellulose accessible surface area, and shows good correlation between enzyme accessibility and enzymatic hydrolysis of pretreated lignocellulosic biomass, while the total dye adsorption accounts for the total accessible surface area (Chandra et al., 2008, 2009). Thus, a modified Simons' staining assay developed previously was used to explore the pore profile and accessibility of milled substrates.

As shown in Table 3, the total dye adsorption (DO and DB) increases with milling time, from 60.6 mg/g for the starting material to 169.2 mg/g for the sample milled for 12 min, suggesting increased total accessibility after mechanical pretreatment. In addition, the orange dye showed a higher adsorption increase than the blue dye for the same milling time, resulting in an increase of O/B ratio, from 0.21(starting material) to 0.54 (sample milled for 12 min). The increased O/B ratio is a direct indication of increased porosity in the micronized wood, which can also be visualized in TEM micrograph (Fig. 4). The increased DO, total dye adsorption and ratio of O/B for micronized wood suggest a significant increase of the accessible surface area and porosity after intense mechanical pretreatment.

3.8. Correlations of structural factors to hydrolysis

For resolving the structural factors behind hydrolysability of micronized wood, its correlations with the determined physicochemical characterizations are summarized in Table 3. The structural factors are correlated with the glucan conversion of micronized wood. However, correlation between the factors themselves is also expected, as the changes in these structural factors during the mechanical milling process is not independent (Jiang et al., 2017b). It is highly required to quantify the relative importance of various factors affecting enzymatic hydrolysis of micronized wood. Principle component analysis (PCA) is a good way to weigh the relative order of multivariate data despite the

Table 3
Correlations between morphological/structural properties and digestibility.

Sample No.	Glucan conversion%	Particle size μm	Degree of polymerization	Crystallinity index/%	Reducing ends	Cellulose accessibility (DO dye adsorption mg/g)	Total accessibility (total dye adsorption mg/g)	Porosity (O/B ratio)
RM0	6.23	756	1068	52.27	16.64	10.48	60.65	0.209
RM2	23.73	115	891	47.9	20.22	17.23	81.38	0.268
RM4	41.35	26.8	565	30.82	28.48	25.94	98.54	0.358
RM6	62.06	21.7	429	22.64	37.46	29.39	107.16	0.38
RM8	77.32	17.9	398	17.32	43.22	39.14	129.1	0.44
RM10	81.77	15.5	324	11.92	50.11	45.29	137.54	0.491
RM12	89.81	15.5	293	8.87	53.96	59.54	169.24	0.543
Correlation coefficient (R^2)		0.56	0.95	0.98	0.97	0.91	0.92	0.96

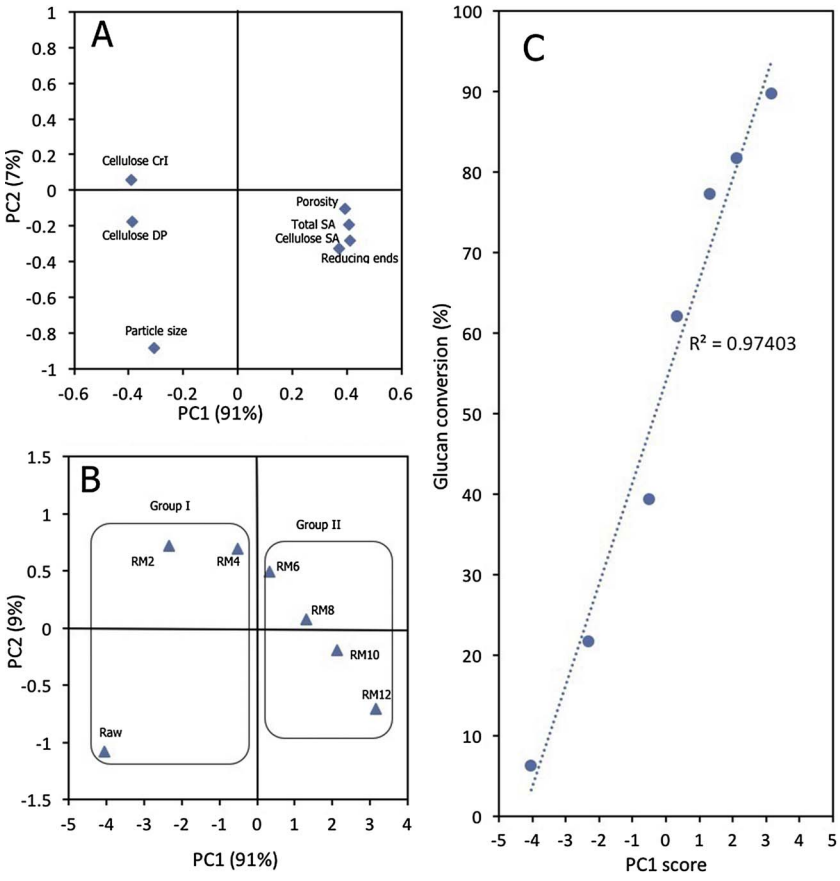

Fig. 6. PCA of correlation of the structural properties of micronized wood: loading plot (A), score plot (B) and correlation between PC1 score and enzymatic glucan conversion (C).

partial collinearity, and the similarity and difference between the factors and between samples can be simply visualized in plots (Pihlajaniemi et al., 2016; Xu et al., 2016). Therefore, PCA was used to elucidate the relative weight of structural factors resulted from mechanical deconstruction on facilitating hydrolysability of micronized wood. The results including loading and score plots are shown in Fig. 6. The loading plot (Fig. 6A) shows that PC1 is negatively related to particle size, cellulose CrI and DPn, while being positively related to reducing ends, cellulose surface accessibility (SA), total surface accessibility (SA) and porosity. Except for particle size, almost all the evaluated variables had high loading values, indicating that they are important factors influencing enzymatic hydrolysis of micronized wood.

Of the variables tested, cellulose CrI had the highest negative effect on glucan conversion, having the highest PC1 loading value of −0.391 (Fig. 6A). This highlights the importance of disruption of crystalline structure of microfibrils for activating wood cellulose with a manner of mechanical action. Disrupting crystal structure of cellulose facilitates accessibility of enzyme, due to the lower physical barrier effect of amorphous cellulose. The glucan conversion was indeed slow down by cellulose crystallinity index as shown in Table 3. Decrease of cellulose crystallinity has been recognized coincidently to occur with disintegration of wood cell wall integrity (i.e. reduction of particle size) during mechanical milling process. Although particle size reduction is the primary physical changes resulted from mechanical deconstruction of biomass, it had the least effect on hydrolysability since it has the lowest PC1 loading value of −0.308 (Fig. 6A). The reason may be attribute to particle aggregation during intensive mechanical milling process. According to previous research on hydrolysis of mechanically pretreated biomass, particle size reduction can predominate increase of cellulose hydrolysis before size reduction to a limit ca. 30 μm, while other physical structure changes in the milled substrates dominate after the particle size limit (Hoeger et al., 2013; Jiang et al., 2016). The little changes in particle size at micrometer range also resulted in its low correlation with glucan conversion (as shown in Table 3).

Although mechanical milling pretreatment did not alter the chemical compositions of micronized wood with different milling times,

mechanical fragmentation broke the β–glycosidic bonds in cellulose chains, since cellulose DP decreases significantly after mechanical pretreatment. The cellulose DP had the second highest negative effect on hydrolysability with PC1 loading value of −0.38 and showed a generally negative correlation with glucan conversion (Table 3). The main function of decreasing cellulose DP is that it increases available reducing ends for endoglucanase attack, thereby weakening the networks to permit better accessibility, subsequently enhancing enzymatic hydrolysis rate and extent (Bali et al., 2015; Kumar et al., 2013). The increase in the values of reducing ends in micronized wood samples also confirmed the degradation of cellulose chains. The reducing end was found to play positive effect on hydrolysability of cellulose, having PC1 loading value of 0.37 (Fig. 6A). These findings collectively demonstrate the important role of fragmenting cellulose chains (i.e., decreasing cellulose DP) to relieve the recalcitrance of native biomass and improve enzymatic hydrolysis of micronized wood.

The most pronounced positive factor was cellulose surface accessibility, showing the largest positive effect on glucan conversion with PC1 loading value of 0.413 (Fig. 6A). It highlights the importance of relieving physical barriers and the kinetic role of the cellulose surface for available reaction site to enzymes. Lignin has been recognized as one of the barriers, which originally encapsulated the cellulose microfibrils in the hierarchical cell wall. Results of CLSM imaging indicates that mechanically fragmenting the fiber cell wall eventually results in a homogeneous redistribution of lignin, decreasing physical barrier effect. The increased orange dye adsorption as measured by Simon's stain technique confirms that redistributing the lignin plays a key role in improving the available/accessible cellulose surface area of micronized wood. Relieving lignin barrier also complements the increased surface area afforded by particle size reduction. In a previous study, Ji et al. (2016) found that redistribution of cellulose in the inner cell wall layers on the surface of particles after destroying the cellular structure of fibers significantly improved the surface area of accessible cellulose, as the O/C ratio revealed by XPS characterization increased significantly for this sample. Several studies have found that lignin migrates and relocates within and/or out of the plant cell walls after thermochemical pretreatments (e.g., dilute acid and AFEX) (Chundawat et al., 2011a,b; Donohoe et al., 2008). The relocalization of lignin caused by phase transition during thermochemical pretreatment process is thought to play important role in providing more accessible cellulose area and facilitating subsequent enzymatic hydrolysis efficiency of pretreated substrates. In this study, results from imaging and dye probing analyses demonstrated that mechanical pretreatment effectively relieves the physical barrier effects of lignin and increases the available cellulose surface area by destroying the highly ordered cell wall structure and coincidently causing redistribution of cell wall compositions.

Another important recalcitrance factor that impedes the efficient enzymatic hydrolysis of cellulose is related to the cell wall heterogeneity and the polymer interaction forming a tightly packed structure. Such packing density physically limits enzyme accessibility to the cellulose molecules (Meng and Ragauskas, 2014). Removing the lignin and/or hemicellulose has been recognized as the leading factor for increasing substrate porosity with chemical or biological approaches (Chiaramonti et al., 2012). TEM imaging reveals a remarkable ultrastructural disruption, providing a substantial accessible surface area by fragmenting the cell wall into fragments and disrupting cellulose microfibrils network (Figs. 3 and 4). The degree of ultrastructure disruption increases with milling time, leading to substantial nanoscale microfibrils aggregates and intra voids in sample with 12-min milling (Fig. 4D). The increase of total dye adsorption and O/B ratio from Simons' staining technique confirmed that mechanical pretreatment caused substantial increase in total surface area and porosity, although the chemical components in the cell wall matrix did not change. Both total surface area and porosity turned to be the second largest factor for glucan conversion, having a PC1 loading value of 0.39 (Fig. 6A). These results also indicate that in addition to changes in cell wall chemistry, deconstruction of cell wall appears to increase porosity and accessible surface area, facilitating subsequent enzymatic hydrolysis. In a study, Wang et al. (Wang et al., 2014) found that the chemical composition of dilute acid pretreated corn stover was similar using three different reactors configurations, however, the enzymatic hydrolysis efficiency of these samples varied significantly. Simon's stain and electronic microscopy analysis revealed that mechanical action in the reactors increased cellulose accessible surface area due to cell wall delamination. The difference in hydrolysability between pretreated biomass samples with the same chemistry indicates that treatments which maximize the substrate accessible surface area dominates over changes in cell wall chemistry.

As shown in Fig. 6B, the difference between the micronized samples was characterized by PC1. The samples could be classified as two groups based on PC1 scores. Group I with PC1 scores less than 0 included samples with short milling time (i.e., Raw, RM2, RM4). These samples were found to be recalcitrant to hydrolysis with relative low glucan conversion. This may attribute to size reduction dominates the structural changes of micronized wood. The other samples in Group II with PC1 scores more than 0 gave high hydrolysability. It is likely that the physical structural changes resulted in increasing surface area and porosity predominately contribute to hydrolysability of micronized wood. Inspired by the above results, PC1 scores was correlated with the glucan conversion (Fig. 6B). There existed strongly linear correlation between glucan conversion and PC1 score (R^2 value of 0.98), indicating the hydrolysability could be simply predicted by a principle component PC1 rather than multivariate.

4. Conclusions

Mechanical milling pretreatment produced micronized wood with significantly different hydrolysability performance but negligible changes in chemical composition. In tandem with particle size reduction, mechanical milling caused multiple deconstruction of cell wall ultrastructure, thereby, creating a highly porous structure with increased accessible surface. Disintegration of cell wall into various fragments coincidently resulted in redistribution of cell wall components and disruption of cellulose, maximizing the surface area of accessible cellulose. The intercorrelated physicochemical properties were converted into a simple combined variable (PC1) to characterize the biomass recalcitrance to hydrolysability by PCA, while cellulose hydrolysability was correlated well with PC1 score. The established weighed order of factors behind enzymatic hydrolysis provides insights of lowering structural recalcitrance by mechanical manner.

Acknowledgements

The authors are grateful to the financial support from the USDA Agriculture and Food Research Initiative (AFRI) Competitive grant (No. 2011-68005-30416), through the Northwest Advanced Renewables Alliance (NARA). The authors would also like to acknowledge the help of image analysis from Franceschi Microscopy & Imaging Center (FMIC) at Washington State University, Pullman.

References

Adney, B., Baker, J., 1996. Measurement of cellulase activities. Lab. Anal. Proced. 6.
Bali, G., Meng, X., Deneff, J.I., Sun, Q., Ragauskas, A.J., 2015. The effect of alkaline pretreatment methods on cellulose structure and accessibility. ChemSusChem 8, 275–279. http://dx.doi.org/10.1002/cssc.201402752.
Barakat, A., de Vries, H., Rouau, X., 2013. Dry fractionation process as an important step in current and future lignocellulose biorefineries: a review. Bioresour. Technol. 134, 362–373. http://dx.doi.org/10.1016/j.biortech.2013.01.169.
Barakat, A., Mayer-Laigle, C., Solhy, A., Arancon, R.A.D., de Vries, H., Luque, R., 2014. Mechanical pretreatments of lignocellulosic biomass: towards facile and environmentally sound technologies for biofuels production. RSC Adv. 4, 48109–48127. http://dx.doi.org/10.1039/C4RA07568D.
Chandra, R., Ewanick, S., Hsieh, C., Saddler, J.N., 2008. The characterization of

pretreated lignocellulosic substrates prior to enzymatic hydrolysis, part 1: a modified Simons' staining technique. Biotechnol. Prog. 24, 1178–1185.
Chandra, R.P., Ewanick, S.M., Chung, P.A., Au-Yeung, K., Rio, L.D., Mabee, W., Saddler, J.N., 2009. Comparison of methods to assess the enzyme accessibility and hydrolysis of pretreated lignocellulosic substrates. Biotechnol. Lett. 31, 1217–1222. http://dx.doi.org/10.1007/s10529-009-9993-5.
Chiaramonti, D., Prussi, M., Ferrero, S., Oriani, L., Ottonello, P., Torre, P., Cherchi, F., 2012. Review of pretreatment processes for lignocellulosic ethanol production, and development of an innovative method. Biomass Bioenergy 46, 25–35. http://dx.doi.org/10.1016/j.biombioe.2012.04.020.
Chundawat, Shishir P.S., Beckham, G.T., Himmel, M.E., Dale, B.E., 2011a. Deconstruction of lignocellulosic biomass to fuels and chemicals. Annu. Rev. Chem. Biomol. Eng. 2, 121–145. http://dx.doi.org/10.1146/annurev-chembioeng-061010-114205.
Chundawat, Shishir P.S., Donohoe, B.S., da Costa Sousa, L., Elder, T., Agarwal, U.P., Lu, F., Ralph, J., Himmel, M.E., Balan, V., Dale, B.E., 2011b. Multi-scale visualization and characterization of lignocellulosic plant cell wall deconstruction during thermochemical pretreatment. Energy Environ. Sci. 4, 973. http://dx.doi.org/10.1039/c0ee00574f.
Del Rio, L.F., Chandra, R.P., Saddler, J.N., 2011. The effects of increasing swelling and anionic charges on the enzymatic hydrolysis of organosolv-pretreated softwoods at low enzyme loadings. Biotechnol. Bioeng. 108, 1549–1558. http://dx.doi.org/10.1002/bit.23090.
Donohoe, B.S., Decker, S.R., Tucker, M.P., Himmel, M.E., Vinzant, T.B., 2008. Visualizing lignin coalescence and migration through maize cell walls following thermochemical pretreatment. Biotechnol. Bioeng. 101, 913–925. http://dx.doi.org/10.1002/bit.21959.
Foston, M., Ragauskas, A.J., 2010. Changes in the structure of the cellulose fiber wall during dilute acid pretreatment in *Populus* studied by ^{1}H and ^{2}H NMR. Energy Fuels 24, 5677–5685. http://dx.doi.org/10.1021/ef100882t.
Fujimoto, A., Matsumoto, Y., Chang, H.-M., Meshitsuka, G., 2005. Quantitative evaluation of milling effects on lignin structure during the isolation process of milled wood lignin. J. Wood Sci. 51, 89–91. http://dx.doi.org/10.1007/s10086-004-0682-7.
Ganner, T., Bubner, P., Eibinger, M., Mayrhofer, C., Plank, H., Nidetzky, B., 2012. Dissecting and reconstructing synergism: in situ visualization of cooperation of cooperativity among cellulase. J. Biol. Chem. 287, 43215–43222. http://dx.doi.org/10.1074/jbc.M112.419952.
Goundalkar, M., Corbett, D., Bujanovic, B., 2014. Comparative analysis of milled wood lignins (MWLs) isolated from sugar maple (SM) and hot-water extracted sugar maple (ESM). Energies 7, 1363–1375. http://dx.doi.org/10.3390/en7031363.
Harmsen, P., Huijgen, W., Bermudez, L., Bakker, R., 2010. Literature Review of Physical and Chemical Pretreatment Processes for Lignocellulosic Biomass. Wageningen UR, Food & Biobased Research.
Himmel, M.E., Ding, S.-Y., Johnson, D.K., Adney, W.S., Nimlos, M.R., Brady, J.W., Foust, T.D., 2007. Biomass recalcitrance: engineering plants and enzymes for biofuels production. Science 315, 804–807. http://dx.doi.org/10.1126/science.1137016.
Hoeger, I.C., Nair, S.S., Ragauskas, A.J., Deng, Y., Rojas, O.J., Zhu, J.Y., 2013. Mechanical deconstruction of lignocellulose cell walls and their enzymatic saccharification. Cellulose 20, 807–818. http://dx.doi.org/10.1007/s10570-013-9867-9.
Holtman, K.M., Chang, H., Jameel, H., Kadla, J.F., 2006. Quantitative ^{13}C NMR characterization of milled wood lignins isolated by different milling techniques. J. Wood Chem. Technol. 26, 21–34. http://dx.doi.org/10.1080/02773810600582152.
Ji, G., Gao, C., Xiao, W., Han, L., 2016. Mechanical fragmentation of corncob at different plant scales: impact and mechanism on microstructure features and enzymatic hydrolysis. Bioresour. Technol. 205, 159–165. http://dx.doi.org/10.1016/j.biortech.2016.01.029.
Jiang, J., Wang, J., Zhang, X., Wolcott, M., 2016. Evaluation of physical structural features on influencing enzymatic hydrolysis efficiency of micronized wood. RSC Adv. 6, 103026–103034. http://dx.doi.org/10.1039/C6RA22371K.
Jiang, J., Wang, J., Zhang, X., Wolcott, M., 2017a. Microstructure change in wood cell wall fracture from mechanical pretreatment and its influence on enzymatic hydrolysis. Ind. Crops Prod. 97, 498–508. http://dx.doi.org/10.1016/j.indcrop.2017.01.001.
Jiang, J., Wang, J., Zhang, X., Wolcott, M., 2017b. Characterization of micronized wood and energy-size relationship in wood comminution. Fuel Process. Technol. 161, 76–84. http://dx.doi.org/10.1016/j.fuproc.2017.03.015.
Ju, X., Grego, C., Zhang, X., 2013. Specific effects of fiber size and fiber swelling on biomass substrate surface area and enzymatic digestibility. Bioresour. Technol. 144, 232–239. http://dx.doi.org/10.1016/j.biortech.2013.06.100.
Kumar, R., Hu, F., Hubbell, C.A., Ragauskas, A.J., Wyman, C.E., 2013. Comparison of laboratory delignification methods, their selectivity, and impacts on physiochemical characteristics of cellulosic biomass. Bioresour. Technol. 130, 372–381. http://dx.doi.org/10.1016/j.biortech.2012.12.028.
Leskinen, T., King, A.W.T., Kilpeläinen, I., Argyropoulos, D.S., 2011. Fractionation of lignocellulosic materials with ionic liquids. 1. Effect of mechanical treatment. Ind. Eng. Chem. Res. 50, 12349–12357. http://dx.doi.org/10.1021/ie200063x.
Li, K., Reeve, D.W., 2005. Fluorescent labeling of lignin in the wood pulp fiber wall. J. Wood Chem. Technol. 24, 169–181.
Liimatainen, H., Sirviö, J., Haapala, A., Hormi, O., Niinimäki, J., 2011. Characterization of highly accessible cellulose microfibers generated by wet stirred media milling. Carbohydr. Polym. 83, 2005–2010. http://dx.doi.org/10.1016/j.carbpol.2010.11.007.
Maurer, A., Fengel, D., 1992. On the origin of milled wood lignin part 1: the influence of ball-milling on the ultrastructure of wood cell walls and the solubility of liginn. Holzforschung 46, 417–423.
Meng, X., Ragauskas, A.J., 2014. Recent advances in understanding the role of cellulose accessibility in enzymatic hydrolysis of lignocellulosic substrates. Curr. Opin. Biotechnol. 27, 150–158. http://dx.doi.org/10.1016/j.copbio.2014.01.014.
Mikushina, I.V., Troitskaya, I.B., Dushkin, A.V., Bazarnova, N.G., 2002. Changes in the chemical composition of wood during mechanochemical treatment. Chem. Sust. Dev. 10, 441–445.
Miller, G.L., 1959. Use of dinitrosalicylic acid reagent for determination of reducing sugar. Anal. Chem. 31, 426–428.
Nge, T.T., Lee, S.-H., Endo, T., 2013. Preparation of nanoscale cellulose materials with different morphologies by mechanical treatments and their characterization. Cellulose 20, 1841–1852. http://dx.doi.org/10.1007/s10570-013-9962-y.
Pihlajaniemi, V., Sipponen, M.H., Liimatainen, H., Sirviö, J.A., Nyyssölä, A., Laakso, S., 2016. Weighing the factors behind enzymatic hydrolyzability of pretreated lignocellulose. Green Chem. 18, 1295–1305. http://dx.doi.org/10.1039/C5GC01861G.
Sant'Anna, C., Costa, L.T., Abud, Y., Biancatto, L., Miguens, F.C., de Souza, W., 2013. Sugarcane cell wall structure and lignin distribution investigated by confocal and electron microscopy: cell wall ultrastructure and lignin localization in sugarcane. Microsc. Res. Tech. 76, 829–834. http://dx.doi.org/10.1002/jemt.22235.
Segal, L., Creely, J.J., Martin Jr, A.E., 1959. An empirical method for estimating the degree of crystallinity of native cellulose using the X-ray diffractometer. Text. Res. J. 29, 786–794.
Silva, G.G.D., Couturier, M., Berrin, J.-G., Buléon, A., Rouau, X., 2012. Effects of grinding processes on enzymatic degradation of wheat straw. Bioresour. Technol. 103, 192–200. http://dx.doi.org/10.1016/j.biortech.2011.09.073.
Singh, S., Simmons, B.A., Vogel, K.P., 2009. Visualization of biomass solubilization and cellulose regeneration during ionic liquid pretreatment of switchgrass. Biotechnol. Bioeng. 104, 68–75. http://dx.doi.org/10.1002/bit.22386.
Sipponen, M.H., Laakso, S., Baumberger, S., 2014. Impact of ball milling on maize (Zea mays L.) stem structural components and on enzymatic hydrolysis of carbohydrates. Ind. Crops Prod. 61, 130–136. http://dx.doi.org/10.1016/j.indcrop.2014.06.052.
Sluiter, A., Hames, B., Hyman, D., Payne, C., Ruiz, R., Scarlata, C., Sluiter, J., Templeton, D., Wolfe, J., 2008a. Determination of total solids in biomass and total dissolved solids in liquid process samples. Natl. Renew. Energy Lab. Colo NREL/TP 510-42621.
Sluiter, A., Hames, B., Ruiz, R., Scarlata, C., Sluiter, J., Templeton, D., Crocker, D., 2008b. Determination of structural carbohydrates and lignin in biomass. Natl. Renew. Energy Lab. Colo NREL/TP 510-42618.
Tadesse, H., Luque, R., 2011b. Advances on biomass pretreatment using ionic liquids: an overview. Energy Environ. Sci. 4, 3913. http://dx.doi.org/10.1039/c0ee00667j.
Takahashi, T., Ito, K., Ito, A., Enda, Y., Gochi, M., Mori, H., Kobayashi, J., 2013. Tandem-ring mill pulverization benefits for enzymatic saccharification of biomass. Renew. Energy. http://dx.doi.org/10.1016/j.renene.2013.07.046.
Vaidya, A.A., Donaldson, L.A., Newman, R.H., Suckling, I.D., Campion, S.H., Lloyd, J.A., Murton, K.D., 2016. Micromorphological changes and mechanism associated with wet ball milling of Pinus radiata substrate and consequences for saccharification at low enzyme loading. Bioresour. Technol. 214, 132–137. http://dx.doi.org/10.1016/j.biortech.2016.04.084.
Wang, W., Chen, X., Donohoe, B.S., Ciesielski, P.N., Katahira, R., Kuhn, E.M., Kafle, K., Lee, C.M., Park, S., Kim, S.H., et al., 2014. Effect of mechanical disruption on the effectiveness of three reactors used for dilute acid pretreatment of corn stover Part 1: chemical and physical substrate analysis. Biotechnol. Biofuels 7, 1–13.
Xu, J., Zong, M.-H., Fu, S.-Y., Li, N., 2016. Correlation between physicochemical properties and enzymatic digestibility of rice straw pretreated with cholinium ionic liquids. ACS Sustain. Chem. Eng. 4, 4340–4345. http://dx.doi.org/10.1021/acssuschemeng.6b00860.
Yang, B., Dai, Z., Ding, S.-Y., Wyman, C.E., 2011. Enzymatic hydrolysis of cellulosic biomass. Biofuels 2, 421–450. http://dx.doi.org/10.4155/bfs.11.116.
Yokoyama, T., Kadla, J.F., Chang, H., 2002. Microanalytical method for the characterization of fiber components and morphology of woody plants. J. Agric. Food Chem. 50, 1040–1044. http://dx.doi.org/10.1021/jf011173q.
Yu, X., Minor, J.L., Atalla, R.H., 1995. Mechanism of action of Simons' stain. Tappi J. 78 175–175.
Yu, Z., Gwak, K.-S., Treasure, T., Jameel, H., Chang, H., Park, S., 2014. Effect of lignin chemistry on the enzymatic hydrolysis of woody biomass. ChemSusChem 7, 1942–1950. http://dx.doi.org/10.1002/cssc.201400042.
Zakaria, M.R., Fujimoto, S., Hirata, S., Hassan, M.A., 2014. Ball milling pretreatment of oil palm biomass for enhancing enzymatic hydrolysis. Appl. Biochem. Biotechnol. http://dx.doi.org/10.1007/s12010-014-0964-5.
Zhang, Z.H., Ji, Z., Ma, J.F., Xu, F., 2012. Anatomy, cell wall ultrastructure and inhomogeneity in lignin distribution of broussonetia papyrifera. Cellul. Chem. Technol. 46, 157–164.
Zhao, X., Zhang, L., Liu, D., 2012. Biomass recalcitrance: part I: the chemical compositions and physical structures affecting the enzymatic hydrolysis of lignocellulose. Biofuels Bioprod. Biorefin. 6, 465–482.
Zhu, J.Y., Pan, X.J., Wang, G.S., Gleisner, R., 2009. Sulfite pretreatment (SPORL) for robust enzymatic saccharification of spruce and red pine. Bioresour. Technol. 100, 2411–2418. http://dx.doi.org/10.1016/j.biortech.2008.10.057.
Zoia, L., King, A.W.T., Argyropoulos, D.S., 2011. Molecular weight distributions and linkages in lignocellulosic materials derivatized from ionic liquid media. J. Agric. Food Chem. 59, 829–838. http://dx.doi.org/10.1021/jf103615e.